SUPPLEMENTAL INFORMATION

Fragment-based discovery of a dual pan-RET/VEGFR2 kinase inhibitor optimized for single-agent polypharmacology

Brendan Frett, Francesca Carlomagno, Maria Luisa Moccia, Annalisa Brescia, Giorgia Federico, Valentina De Falco, Brittany Admire, Zhongzhu Chen, Wenqing Qi, Massimo Santoro, and Hong-yu Li**

TABLE OF CONTENTS

Molecular Modelling
A VEGFR-2 DFG-out crystal structure (PDB# 2OH4) and the amino acid sequence of RET (PDB# 2IVU) were obtained. Using SWISS-MODEL Automatic Modelling Mode (swissmodel.expasy.org), the RET sequence was employed to build a RET DFG-out homology model using the VEGFR2 DFG-out structure as a template. Using AutoDock Tools: 1) all hydrogens were added as 'Polar Only'; 2) a grid box for the ATP binding site was created (center x = -25.881, center y = 9.55, center z = -10.927 / size x = 16, size y = 44, size z = 18). Compounds to be computationally modeled were assigned appropriate rotatable bonds using AutoDock Tools. Then, AutoDock Vina was employed to computational model the compounds. The modeling results were visualized and analyzed with Discovery Studio 3.5.

General Chemistry Procedures
All solvents were reagent grade or HPLC grade and all starting materials were obtained from commercial sources and used without further purification. Purity of final compounds was assessed using a Shimadzu ultra-high throughput LC/MS system (SIL-20A, LC-20AD, LC-MS 2020, Phenomenex® Onyx Monolithic C-18 Column) at variable wavelengths of 254 nM and 214 nM (Shimadzu PDA Detector, SPD-MN20A) and was >95%, unless otherwise noted. The HPLC mobile phase consisted of a water-acetonitrile gradient buffered with 0.1% formic acid. ^{1}H NMR spectra were recorded at 400 MHz and ^{13}C spectra were recorded at 100 MHz, both completed on a Varian 400 MHz instrument (Model# 4001S41ASP). Compound activity and kinetics were determined with the EZ Reader II plate reader (PerkinElmer®, Walthman, USA). All compounds were purified using silicagel (0.035-0.070 mm, 60 Å) flash chromatography, unless otherwise noted. Microwave assisted reactions were completed in sealed vessels using a Biotage Initiator microwave synthesizer.

Synthesis: See Supplemental Figure 2 for Synthetic Scheme
Synthesis of ethyl 2-(4-((4-bromo-2-nitrophenyl)amino)phenyl)acetate, **6**. Ethyl 4-aminophenyl acetate, **5**, (3.67 g, 20.45 mmol) was added to a 20 mL microwave vial along with 4-bromo-1-fluoro-2-nitrobenzene (3.00 g, 13.64 mmol) and DMA (10 mL). The reaction was sealed and placed under microwave irradiation for 30 minutes at 160 °C. The crude reaction was added to water and extracted with EtOAc. The organic extract was washed with brine 1X, acidified water (pH ~4) 2X, and brine 2X. The organic layer was collected, dried with $MgSO_4$, and adsorbed on silica. The reaction was purified using flash chromatography with hexanes/EtOAc to afford **6** as blood-red oil that eventually solidified (4.2 g, 81%). ^{1}H NMR (400 MHz, Chloroform-d) δ 9.41 (s, 1H), 8.34 (d, J = 2.4 Hz, 1H), 7.41 (ddd, J = 9.2, 2.4, 0.6 Hz, 1H), 7.34 (d, J = 8.3 Hz, 2H), 7.21 (d, J = 8.3 Hz, 2H), 7.10 (d, J = 9.2 Hz, 1H), 4.18 (q, J = 7.2 Hz, 2H), 3.63 (s, 2H), 1.28 (t, J = 7.2 Hz, 3H). ESIMS m/z [M+H]+ 379.

Synthesis of ethyl 2-(4-((2-amino-4-bromophenyl)amino)phenyl)acetate, **7**. Compound **6** (2.03 g, 5.35mmol) was placed into a 250 mL round bottom flask. EtOH (80 mL) and zinc (2.450 g, 37.5 mmol) were added to the flask and the reaction was placed in an ice bath. Acetic acid (2.145 mL, 37.5 mmol) diluted with EtOH (40 mL) was added dropwise to the reaction over the course of 1 hour. After the addition, the reaction was stirred at 0 °C for 5 hours. The reaction was filtered and EtOH was evaporated. The reaction was slowly basified with aqueous $NaHCO_3$ and extracted with diethyl ether. The reaction was washed 3X with aqueous $NaHCO_3$ and the organic layer was collected, dried with $MgSO_4$, and evaporated to yield **7** as a slight purple solid (1.834 g, 98%). ^{1}H NMR (400 MHz, Chloroform-d) δ 7.12 (d, *J* = 8.5 Hz, 2H), 6.95 (d, *J* = 8.3 Hz, 1H), 6.92 (d, *J* = 2.2 Hz, 1H), 6.83 (dd, *J* = 8.3, 2.2 Hz, 1H), 6.67 (d, *J* = 8.5 Hz,

2H), 5.07 (s, 1H), 4.14 (q, *J* = 7.1 Hz, 2H), 3.82 (s, 2H), 3.51 (s, 2H), 1.25 (t, *J* = 7.1 Hz, 3H). ESIMS *m/z* $[M+H]^+$ 349.

***Synthesis of ethyl 2-(4-(5-bromo-1H-benzo[d]imidazol-1-yl)phenyl)acetate,* 8**. Compound **7** (2.01 g, 5.76 mmol) was added to a 150 mL round bottom flask followed by TMOF (50 mL) and a stir bar. After, pTSA (59.6 mg, 0.314 mmol) was added and the reaction was stirred at room temperature for about an hour or until complete conversion based on TLC. After complete consumption of the starting material, the reaction was extracted with EtOAc and washed with $NaHCO_3$ 3X and brine 3X. The organic layer was collected, dried with $MgSO_4$, and condensed to yield **8** as a brown solid (2.04 g, 99%). ^{1}H NMR (400 MHz, Chloroform-d) δ 8.08 (s, 1H), 8.02 (dd, J = 1.7, 0.6 Hz, 1H), 7.51 (d, J = 8.7 Hz, 2H), 7.47 – 7.42 (m, 3H), 7.39 (dd, J = 8.7, 0.6 Hz, 1H), 4.21 (q, J = 7.1 Hz, 2H), 3.72 (s, 2H), 1.30 (t, J = 7.1 Hz, 3H). ESIMS m/z [M+H]+ 359.

***Synthesis of ethyl 2-(4-(5-bromo-1H-benzo[d]imidazol-1-yl)phenyl)acetate,* 9**. Compound **8** (50 mg, 0.139 mmol) was placed into a 5 mL microwave vial along with 4:1 DMF/Water (2 mL). 1-methyl-4-(4,4,5,5-tetramethyl-1,3,2-dioxaborolan-2-yl)-1H-pyrazole (37.6 mg, 0.181 mmol) was added to the vial along with Na_2CO_3 (73.8 mg, 0.696 mmol). The reaction vessel was degassed for 10 minutes with N_2, followed with the addition of $Pd_2(dba)_3$ (1.274 mg, 0.001 mmol) and $P(Cy)_3$ (1.169 mg, 0.004 mmol). The reaction vessel was sealed under N_2 and microwaved at 120 ˚C for 30 minutes. After, the solvent was evaporated and the crude product was adsorbed onto silica and purified using flash chromatography with a DCM/MeOH gradient. **9** was collected as a white solid (38.1 mg, 76%). ESIMS m/z [M+H]+ 361.

Synthesis of N-(5-(tert-butyl)isoxazol-3-yl)-2-(4-(5-(1-methyl-1H-pyrazol-4-yl)-1H-benzo[d]imidazol-1-yl)phenyl)acetamide, Pz-1 (**4**). **9** (365.3 mg, 1.014 mmol) was dissolved in 1:1 THF/Water (8 mL). LiOH monohydrate (128 mg, 3.04 mmol) was then added to the reaction and the reaction was heated under microwave irradiation for 15 minutes at 100 °C. The reaction was subsequently acidified to a pH ~3-4 and extracted 5X with 4:1 chloroform/IPA. The organic layer was dried with $MgSO_4$ and condensed to yield the acid**, 9a** (302 mg, 90%). The acid (45 mg, 0.135 mmol) was added to a 5 mL vial. Anhydrous DCM (1 mL) was added to the vial, followed by EDC (52.5 mg, 0.338 mmol), HOAt (18.41 mg, 0.135 mmol), and DIPEA (0.028 mL, 0.162 mmol). 5-(tert-butyl)isoxazol-3-amine (29.4 mg, 0.203 mmol) was added and the reaction was sealed under N_2 and was reacted for 12 hours or until complete product conversion. The reaction was quenched with water, extracted with 4:1 Chloroform/IPA, and washed with saturated $NaHCO_3$ 5X. The organic layer was collected, dried with $MgSO_4$, adsorbed onto silica, and purified by flash chromatography using DCM/MeOH to generate Pz-1 (**4**) (44.2 mg, 71.8%). ^{1}H NMR (400 MHz, Chloroform-d) δ 9.91 (s, 1H), 8.10 (s, 1H), 7.95 (d, J = 1.4 Hz, 1H), 7.81 (d, J = 0.6 Hz, 1H), 7.65 (s, 1H), 7.59 (d, J = 8.4 Hz, 2H), 7.51 (d, J = 8.6 Hz, 3H), 7.45 (dd, J = 8.5, 1.4 Hz, 1H), 6.77 (s, 1H), 3.97 (s, 3H), 3.90 (s, 2H), 1.36 (s, 9H). ^{13}C NMR (101 MHz, Chloroform-d) δ 181.94, 168.84, 158.07, 144.61, 142.66, 136.81, 135.57, 134.13, 132.41, 131.06, 127.92, 126.92, 124.25, 123.49, 122.14, 117.04, 110.75, 93.57, 43.40, 39.11, 33.11, 28.65. ESIMS m/z [M+H]+ 455. LC-MS Purity, >95%.

Synthesis of **1**, **1a**, **2**, **3**, **3a** and **3b**. All analogues have been synthesized utilizing a modified procedure to that of Pz-1.

RET biochemical inhibition and kinetic assays

Kinase activity was measured in a microfluidic assay that monitors the separation of a phosphorylated product from substrate. The assay was run using a 12-sipper chip on a Caliper EZ Reader II (PerkinElmer®, Walthman, USA) with separation buffer (100 mM HEPES, 10 mM

EDTA, 0.015% Brij-35, 0.1% CR-3 PerkinElmer®). In 96-well polypropylene plates (Greiner, Frickenhausen, Germany) compound stocks (20 mM in DMSO) were diluted into kinase buffer (50 mM HEPES, 0.075% Brij-35, 0.1 % Tween 20, 2 mM DTT, 10 mM $MgCl_2$, and 0.02% NaN_3) in 12-point ½log dilutions (2 mM–6.32 nM). After, 1 µL was transferred into a 384-well polypropylene assay plate (Greiner). The RET enzyme (Invitrogen™, Grand Island, USA) was diluted in kinase buffer to a concentration of 2 nM and 5 µL of the enzyme mixture was transferred to the assay plate. RET kinase was pre-incubated with the small molecule inhibitor or control buffer, with gentle shaking for 60 min to allow the inhibitor to trap the DFG-out conformation; it has been reported for the Type-II (DFG-out) p38 inhibitor, BIRB-796, that an increase in incubation time increases activity (Pargellis, *et al.* 2002). A substrate mix was prepared containing ATP (Ambresco®, Solon, USA) and tagged RET peptide (peptide #22, 5' FAM-EPLYWSFPA, PerkinElmer®, Walthman, USA) dissolved in kinase buffer, and 5 µL of the substrate mix was added to the assay plate. Running concentrations were as follows: ATP (190 µM), peptide (1.5 µM), compound 12-point ½log dilutions (0.2 mM–0.632 nM). For positive control, no inhibitor was added. For negative control, no enzyme was added. The plate was run until 10-20% conversion based on the positive control wells. The following separation conditions were utilized: upstream voltage -500V; downstream voltage, -1900V; chip pressure -0.8. Percent inhibition was measured for each well comparing starting peptide to phosphorylated product peaks relative to the baseline. Dose response curves, spanning the IC_{50} dose, were generated in GraphPad Prism 6 and fit to an exponential one-phase decay line and IC_{50} values were obtained from the half-life value of the curve. IC_{50} values were generated in triplicate and error was calculated from the standard deviation between values.

For kinetic the assay, compound **3b** was incubated with the RET kinase for 60 minutes and then exposed to a substrate mix containing 100 µM, 50 µM, 12.5 µM, or 6.2 µM ATP. For K_m determination no inhibitor was used. After 20% conversion at the highest ATP concentration, activity at each concentration of ATP was determined in triplicate. Kinetic data was analyzed with GraphPad Prism 6 and fit to an Enzyme kinetics – Substrate vs. Velocity Michaelis-Menten nonlinear regression.

Cell Cultures

Human medullary thyroid carcinoma (MTC) TT cells from American Type Culture Collection (ATCC, Rockville, MD) were grown in RPMI (Roswell Park Memorial Institute) 1640 supplemented with 16% fetal bovine serum (FBS) (Invitrogen, Carlsbad, CA, USA). Human MTC MZ-CRC-1 cells were kindly provided by R.F. Gagel (MD Anderson, Houston, TX) and grown in Dulbecco's Modified Eagle Medium (DMEM) (Invitrogen) supplemented with 10% FBS. Human papillary thyroid carcinoma (PTC) TPC-1 cells were kindly provided by M. Nagao (National Cancer Center Research Institute, Tokyo, Japan) and grown in DMEM with 10% FBS. HeLa cells from ATCC were grown in DMEM with 10% FBS. Immortalized human thyroid cells (Nthy-ori 3-1) were obtained from European Collection of Cell Cultures (ECACC) (Wiltshire, UK) and were grown in RPMI 1640 with 10% FBS. Human NSCLC Lc-2/ad cells were obtained from Sigma-Aldrich (Milano, Italy) and grown in RPMI 1640:HAMS F12 (1:1) with 10% FBS (Matsubara, 2012). HEK293 cells from ATCC were grown in DMEM with 10% FBS; HEK293 cells were transiently transfected with the FuGENE HD reagent according to manufacturer's instructions (Roche, Mannheim, Germany). NIH3T3 (Santoro *et al.*, 1995) and RAT1 (Pasini *et al.,* 1997) fibroblasts expressing different RET point mutants have been described previously. NIH3T3 cells were grown in DMEM with 5% calf serum. RAT1 cells were grown in RPMI 1640 with 10% FBS. HUVECs (Human primary Umbilical Vein Endothelial Cell) were obtained from Lonza (Allendale, NJ) and cultured in Endothelial Cell Growth Medium (CC-3124). Murine interleukin-3 (IL-3) dependent pro-B Ba/F3 cells were from ATCC. Ba/F3 cells stably expressing NCOA4-RET (RET/PTC3) protein were generated by transfecting long isoform (RET-51) of NCOA4-RET by electroporation. Parental and Ba/F3-NCOA4-RET cells were cultured in RPMI

1640 with 10% FBS; parental cells required supplementation with 10 ng/ml IL-3. All cell culture media were supplemented with 2 mM L-glutamine and 100 units/ml penicillin-streptomycin (Invitrogen).

Plasmids. pBabe-based vectors encoding rearranged CCDC6-RET (RET/PTC1) and NCOA4-RET (RET/PTC3) oncogenes were described previously (Melillo *et al.*, 2005). KIF5B-RET cDNA (variant 2) was cloned in pBABE by fusing the 5'-terminal portion of KIF5B cDNA fragment (exons 1-16, encoding residues 1-638) to the 3'-terminal portion of RET cDNA (exons 12-20: encoding residues 713-1072, including the tyrosine kinase domain) (Kohno *et al.*, 2012). Plasmids encoding human VEGFR2/KDR were provided as a kind gift from S. De Falco (IGB, Napoli, Italy).

Protein Studies. Cells were harvested in lysis buffer (50 mM Hepes, pH 7.5, 150 mM NaCl, 10% glycerol, 1% Triton X-100, 1 mM EGTA, 1.5 mM $MgCl_2$, 10 mM NaF, 10 mM sodium pyrophosphate, 1 mM Na_3VO_4, 10 µg of aprotinin/ml, 10 µg of leupeptin/ml) and centrifuged at 10,000 x *g*. Protein concentration was estimated with a modified Bradford assay (Bio-Rad Laboratories, Berkeley, CA, USA). Antigens were detected by an enhanced chemiluminescence detection kit (ECL, Amersham Pharmacia Biotech). Anti-RET is a polyclonal antibody raised against the tyrosine kinase protein fragment of human RET. Anti-pY905 and anti-pY1062 are phospho-specific affinity-purified polyclonal antibodies that recognize RET proteins phosphorylated at Y905 and Y1062, respectively (Carlomagno *et al.,* 2002). Antibodies for VEGFR2/KDR (#2479), p70 S6 kinase (p70S6K) (#2708), and MAPK (ERK) (#9101) were purchased from Cell Signaling (Beverly, MA). Anti-SHC (#H-108) was purchased from Santa Cruz Biotechnology (Santa Cruz, CA). Anti-phospho-SHC (Y317) (#07-206) was purchased from Upstate Biotechnology Inc. (Lake Placid, NY, USA). Other phosphorylation specific antibodies were purchased from Cell Signaling as follows: VEGFR2/KDR (pY1175) (#2478), VEGFR2/KDR (Y1059) (# 3817), MAPK (ERK) (T302/Y304) (#9102), p70 S6 kinase (T389) (#9234) and S6RP (S235/S236) (#4858). Anti-α-tubulin was from Sigma Aldrich (St Louis, MO, USA).

Mouse experiments

Animals were fed *ad libitum* on an autoclaved diet with tap water and maintained at the Dipartimento di Medicina Molecolare e Biotecnologie Mediche Animal Facility in accordance with Italian regulations for experimentation on animals. All manipulations were performed while animals were under anesthesia.

For mouse fibroblast xenografts, NIH3T3 RET/C634Y (200,000) or NIH3T3 HRAS/G12V (50,000) were injected subcutaneously into the dorsal portion (both sides) of 6-week-old female BALB/c nu/nu mice (31 mice/cell line) (Jackson Laboratories, Bar Harbor, Maine). After 4 days, before tumor formation, animals were randomly assigned to receive Pz-1 (1.0, 3.0 or 10 mg/kg daily) (23 mice: 8 mice/group for 1.0 and 3.0 mg/kg daily doses and 7 mice for 10 dose mg/kg daily) by oral gavage or left untreated (8 mice).

Tumor diameters were measured with calipers every 1-2 days. Tumor volumes (V) were calculated by the rotational ellipsoid formula: $V = A \times B^2/2$ (A=axial diameter; B= rotational diameter) and reported as average volumes ± standard deviations (SD). Tumor protein phosphorylations were assayed according to standard Western blot procedures.

Statistical Analysis

To compare *in vitro* cell growth, Student's unpaired *t* test was performed using the Instat software program (Graphpad Software Inc). All *p*-values were two-sided, and differences were statistically significant at $p < 0.02$, unless otherwise noted. IC_{50} doses were calculated through a curve fitting analysis from last day of growth curves using the PRIZM program (GraphPad

Software Inc). To compare tumor growth, Kruskal-Wallis test (non papametric ANOVA) and Dunn's Multiple Comparison test (InStat program, GraphPad Software) were used. *P*-values were statistically significant at $p < 0.05$, unless otherwise noted.

Toxicity

The dose escalation study of Pz-1 was completed at the University of Arizona Pathology Services Laboratory. Twelve male BALB/c mice, 6-8 weeks old, were utilized. Pz-1 was prepared as a suspension employing water (80%), Tween 20 (20%), and xanthan gum (0.05%) at concentrations of 10.0 mg/kg, 30.0 mg/kg, and 100.0 mg/kg. Pz-1 was dosed PO per day for seven days at indicated concentrations to 4 mice at each dose. After the seven days, serum chemistry was completed to monitor levels of ALP (alkaline phosphatase), glucose, ALT (alanine aminotransferase), total serum proteins, albumin, globulin, BUN (blood urea nitrogen), and phosphorus.

Pharmacokinetics

The pharmacokinetic profile of Pz-1 was determined in plasma following a single intravenous (IV) bolus and oral gavage administration to 6 male Sprague-Dawley (SD) rats. The SD rats were 7-9 weeks old, 200-300 grams, and obtained from SLAC Laboratory Animal Co. Ltd., Shanghai, China. Before dosing, SD rats were fasted for 18 hours and then fed ad libitum 4 hours post dosing. Three SD rats for IV injections were surgically indwelled with catheters in both carotid artery (for sampling) and jugular vein (for dosing) using polypropylene tubing and heparin (50 i.u./mL)/glucose (50%) as the lumen lock solution. Three SD rats for oral dosing were surgically implanted with catheters in carotid artery (for sampling) using polypropylene tubing and heparin (50 i.u./mL)/glucose (50%) as the lumen lock solution. The IV dose was formulated with EtOH/PEG400/Water (10:70:20) and the oral dose was formulated with 10% Tween 80. Samples were obtained at 1, 2, 4, 8, and 24 hours post dosing, transferred into plastic microcentrifuge tubes containing 4 µL of K2-EDTA (0.5M) as anti-coagulant and placed on wet ice until centrifugation. Harvested blood samples were centrifuged shortly after collection at 4,000 g 4 °C for 10 minutes. After centrifugation, the amount of Pz-1 in the plasma was determined using LC-MS/MS analysis. Plasma concentration versus time data was analyzed by non-compartmental approaches using the WinNonlin software program (Phoenix®, version 6.2.1, Pharsight, Mountain View, CA). The entire pharmacokinetic study was outsourced to WuXi AppTec (Shanghai) Co., Ltd.

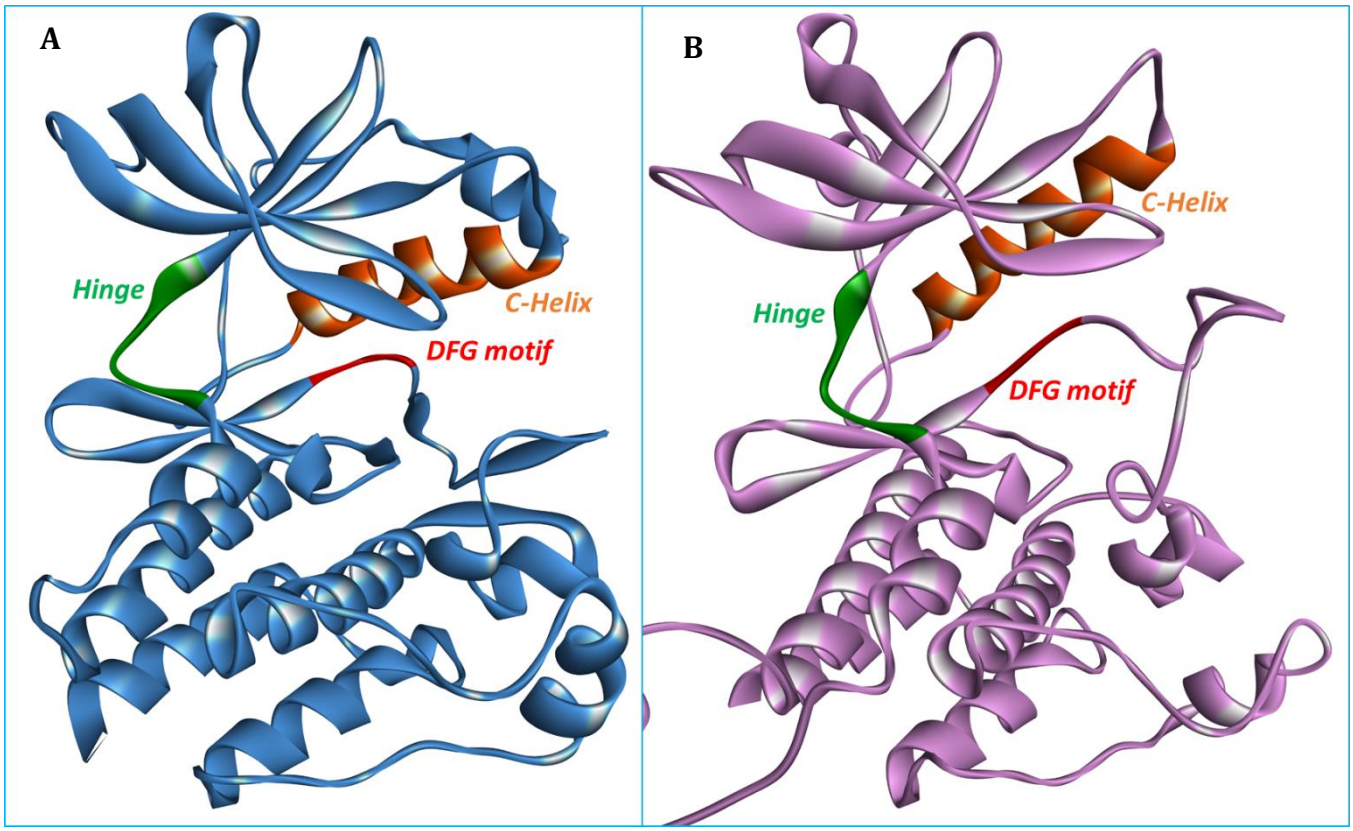

Supplemental Figure 1: Modeling DFG-in and –out conformations of RET kinase.
A) RET DFG-in crystal structure (PDB# 2IVU). Type-I TKIs can bind to this structure. **B**) RET DFG-out homology model created with SWISS-MODEL and a DFG-out template (PDB# 2OH4). The C-helix region is pushed-up and the DFG motif is pushed-out. The movement of both regions opens-up the allosteric pocket, allowing Type-II inhibitors, such as Pz-1, to bind with high affinity.

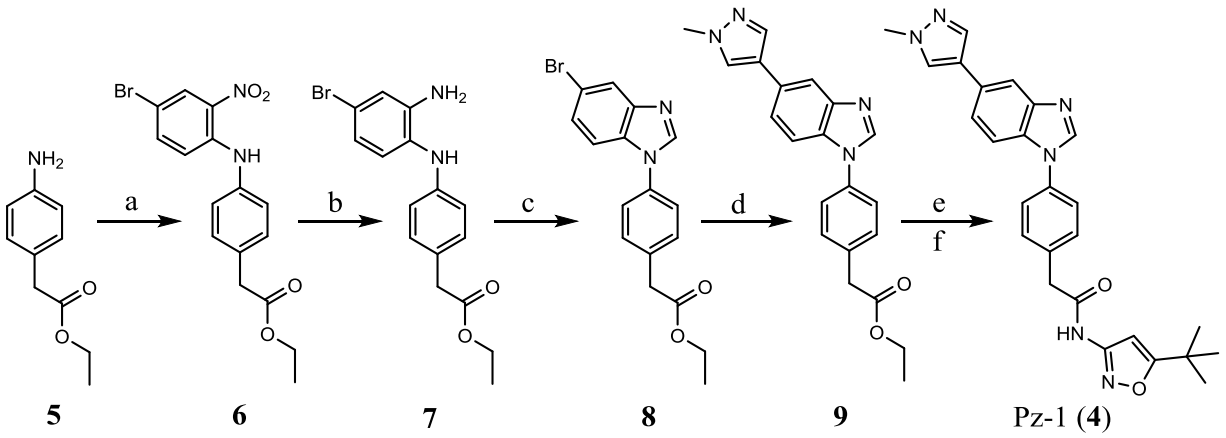

Supplemental Figure 2: Schematic representation of Pz-1 (compound 4) synthesis.

Pz-1 was synthesized using the procedures outlined in the Figure. Briefly, a direct nucleophic substitution on commercially available 4-bromo-1-fluoro-2-nitrobenzene with an aniline (**5**) produced compound **6**. Selective reduction of compound **6**, followed by the cyclization with TMOF, furnished a benzimidazole intermediate (**8**). Methyl pyrazole was added to the 5-position of the benzimidazole with a Suzuki reaction to afford compound **9**. The hydrolysis of compound **9**, followed by amide-bond formation using commercially available 5-(tert-butyl)isoxazol-3-amine, produced Pz-1. The overall yield for six steps was around 20% and Pz-1 could be produced in high (>95%) purity.

a) 4-bromo-1-fluoro-2-nitrobenzene, 160 ˚C, 30 min, MWI, 81%; b) EtOH, Zinc, HOAc, 0 ˚C, 98%; c) TMOF, pTSA, RT, 99%; d) 1-methyl-4-(4,4,5,5-tetramethyl-1,3,2-dioxaborolan-2-yl)-1H-pyrazole, Na_2CO_3, $Pd_2(dba)_3$, $P(Cy)_3$, 120 ˚C, 30 min, MWI, 76%; e) LiOH, 1:1 THF/Water, 100 ˚C, 15 min, MWI. f) EDC, HOAt, DIPEA, 5-(tert-butyl)isoxazol-3-amine, DCM, RT, 12 hr, 72% for two steps from compound **8**.

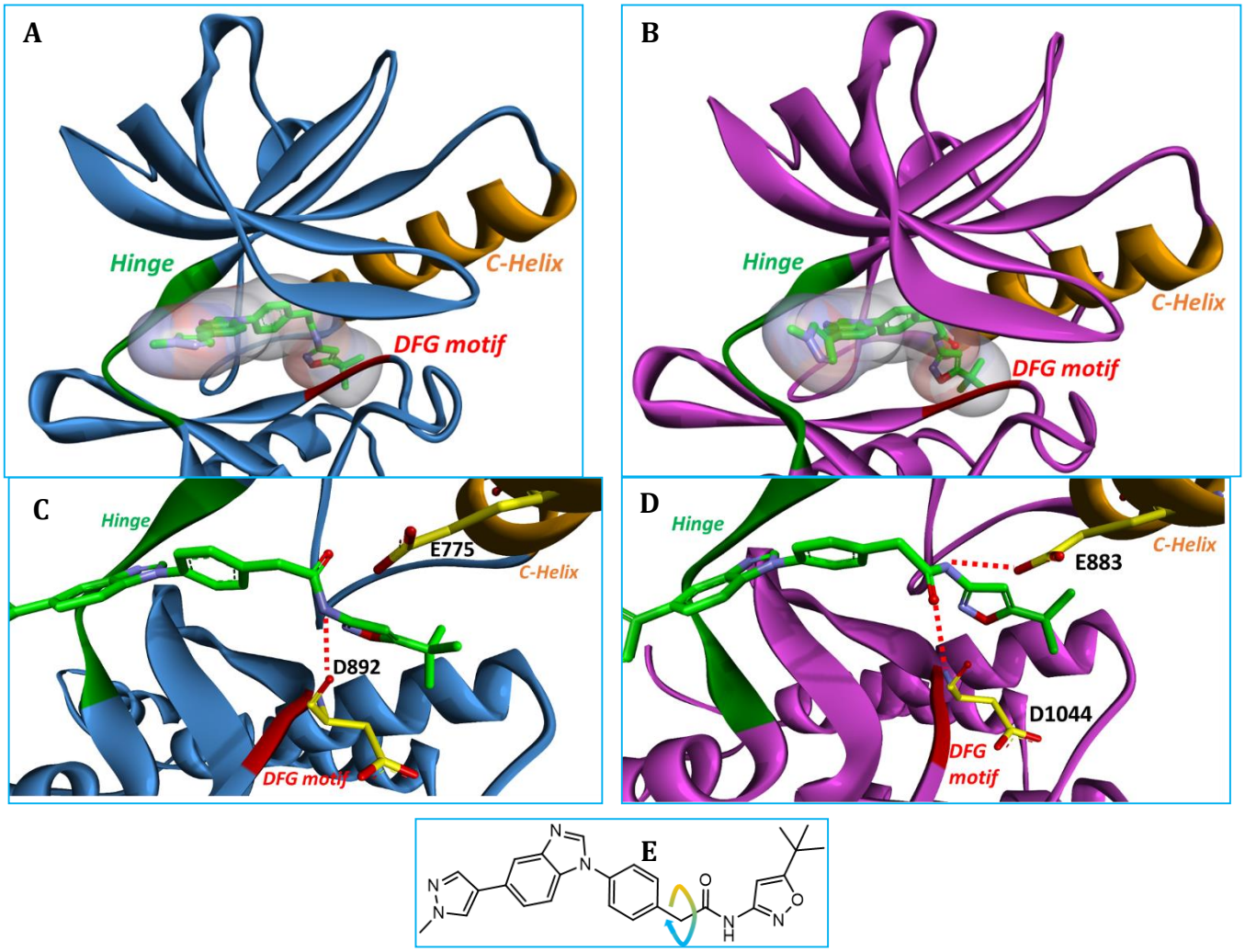

Supplemental Figure 3. Docking models of Pz-1

Docking models of Pz-1 in RET (blue, **A**) and VEGFR2 (pink, **B**). Pz-1 is predicted to take on different binding geometries in each kinase, though their fold and architecture are quite similar. This depends on the free rotation of the methylene linker bridging the hinge region with the allosteric pocket. In RET, the methylene linker positions the amide 'up' (**C**), while in VEGFR2 the linker positions the amide 'down' (**D**). This free rotation presumably helps the inhibitor to achieve equipotency on RET and VEGFR2 because the hydrogen bond contact at either the DFG motif and/or the C-helix can always be maintained.

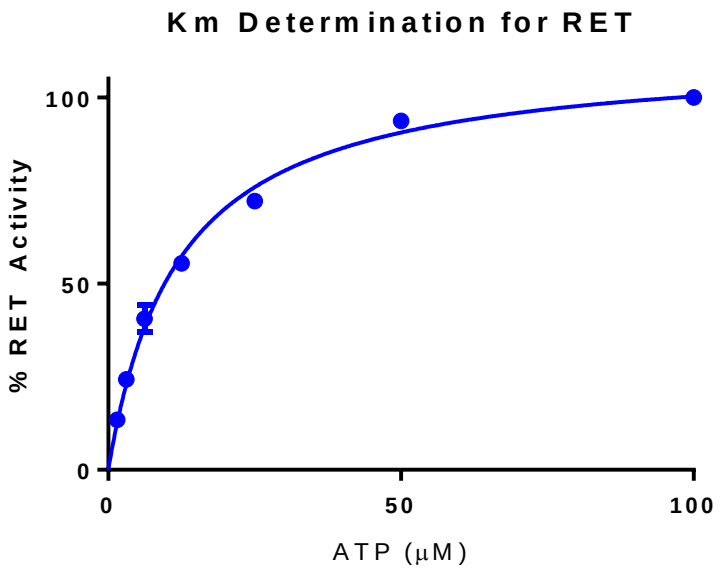

Supplemental Figure 4. Determination of RET K_m for ATP.
The K_m value for RET was 12.00 ± 0.26 μM. Calulcation of the K_m was completed in duplicate.

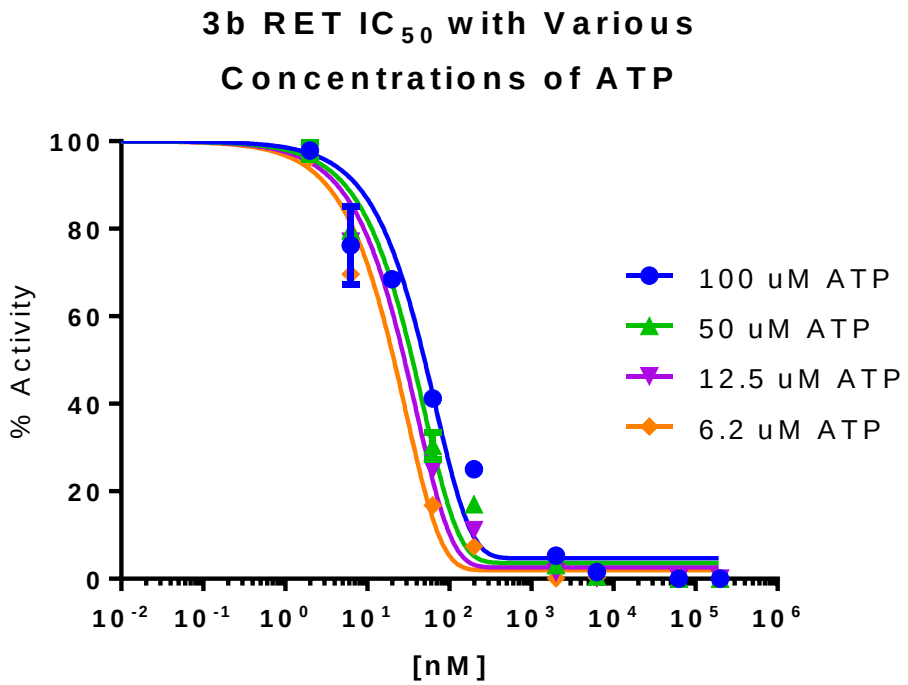

Supplemental Figure 5. RET kinase assay with compound 3b and various concentration of ATP.

100 µM ATP, IC_{50} = 46.5 ± 6.9 nM; 50 µM ATP, IC_{50} = 33.7 ± 3.18; 12.5 µM ATP, IC_{50} = 27.4 ± 1.1 nM; 6.2 µM ATP, IC_{50} = 20.6 ± 4.3 nM. IC_{50} values were determine in triplicate.

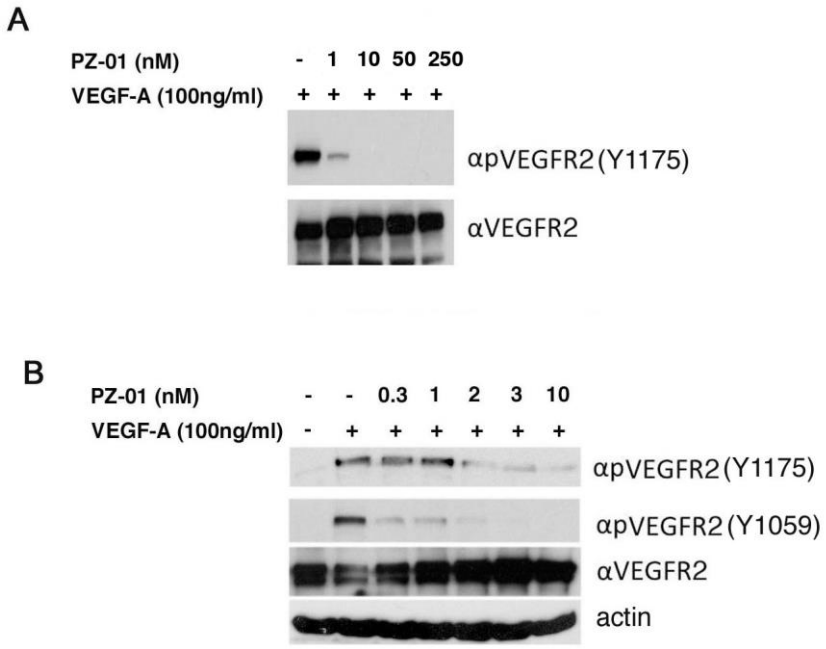

Supplemental Figure 6: VEGFR2 inhibitory activity of Pz-1 in intact cells.

A) HEK293 cells were transiently transfected with human VEGFR2; 36 hr after transfection, cells were serum starved for 12 hr. The indicated doses of Pz-1 or vehicle (-) were added for 2 hr and then VEGFA (100 ng/ml) stimulation was applied for 15 min. **B)** HUVEC cells were kept for 3 hr in EBM (Endothelial Basal Medium) containing 1% FBS, treated for 2 hr with indicated doses of Pz-1 or vehicle (-) and, at the end, stimulated for 10 min or not with VEGFA (100 ng/ml). Cell lysates were immunoblotted with indicated antibodies.

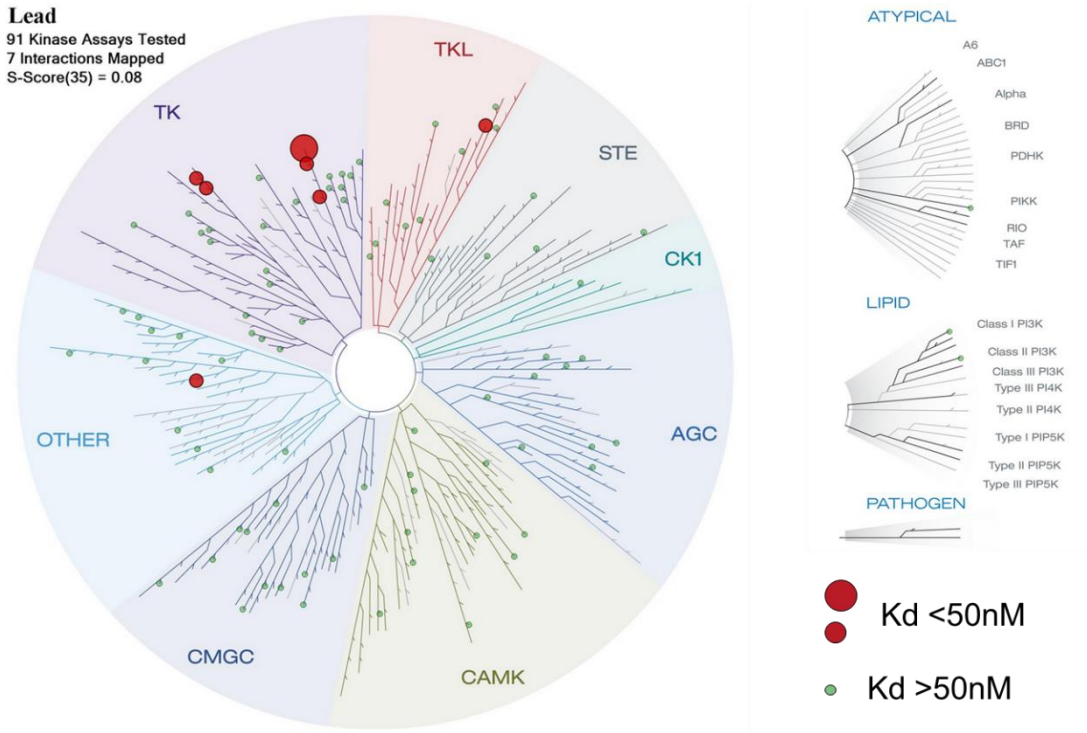

Supplemental Figure 7. Kinome screen.
Pz-1 was screened against a 91 kinase panel at a concentration of 50 nM. RET and VEGFR2 were not included in the screen because Pz-1 inhibition of both of them was already determined to feature an IC_{50} below 1 nM.

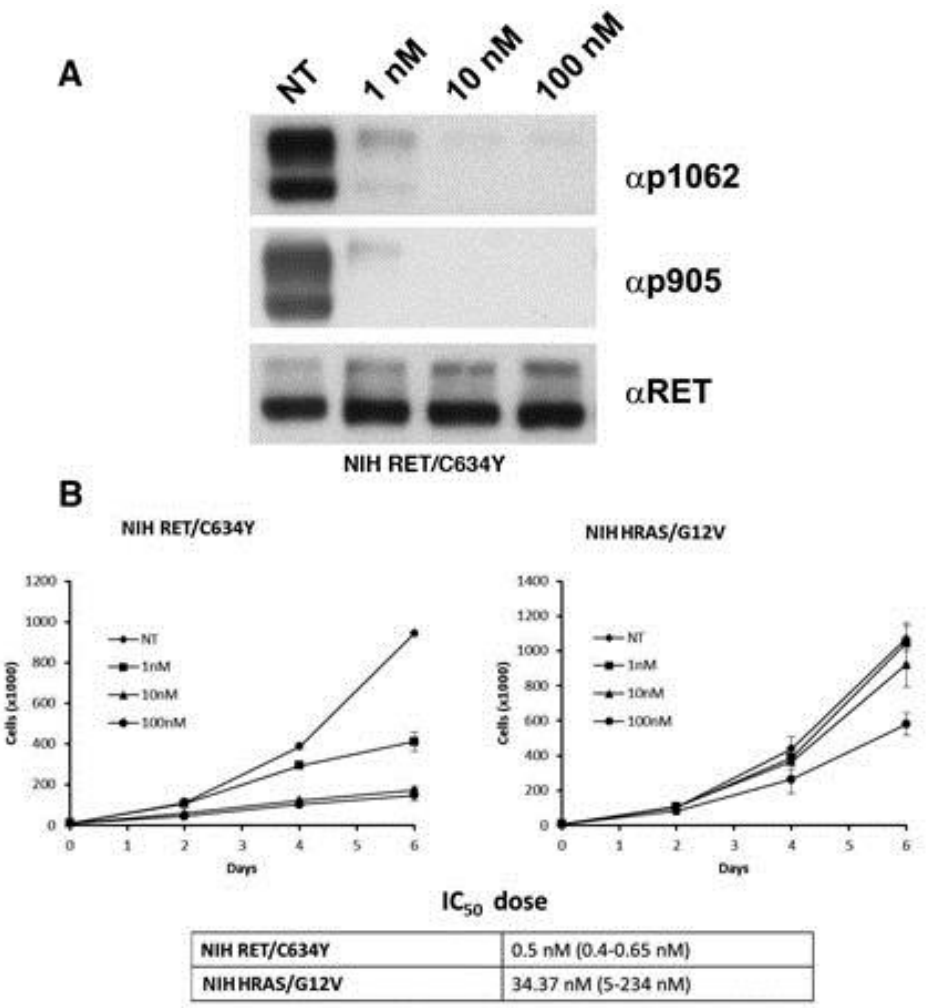

Supplemental Figure 8: Activity of Pz-1 on the proliferation of RET or RAS transformed NIH3T3 cells.

A) Serum-starved NIH3T3-RET/C634Y were treated for 2 hr with increasing concentrations of Pz-1 or vehicle (NT); cell lysates (50 μg) were immunoblotted with phospho-Y1062 (αp1062) or -Y905 (αp905) RET or anti-RET (αRET) antibodies for normalization. **B)** RET/C634Y- or HRAS/G12V-transformed NIH3T3 fibroblasts were incubated with vehicle (NT: not treated) or the indicated concentrations of Pz-1 in 2% serum and counted at the indicated time points. Data are the mean ± SD of one experiment performed in triplicate. Growth inhibition IC50 (with 95% CI) is indicated at the bottom.

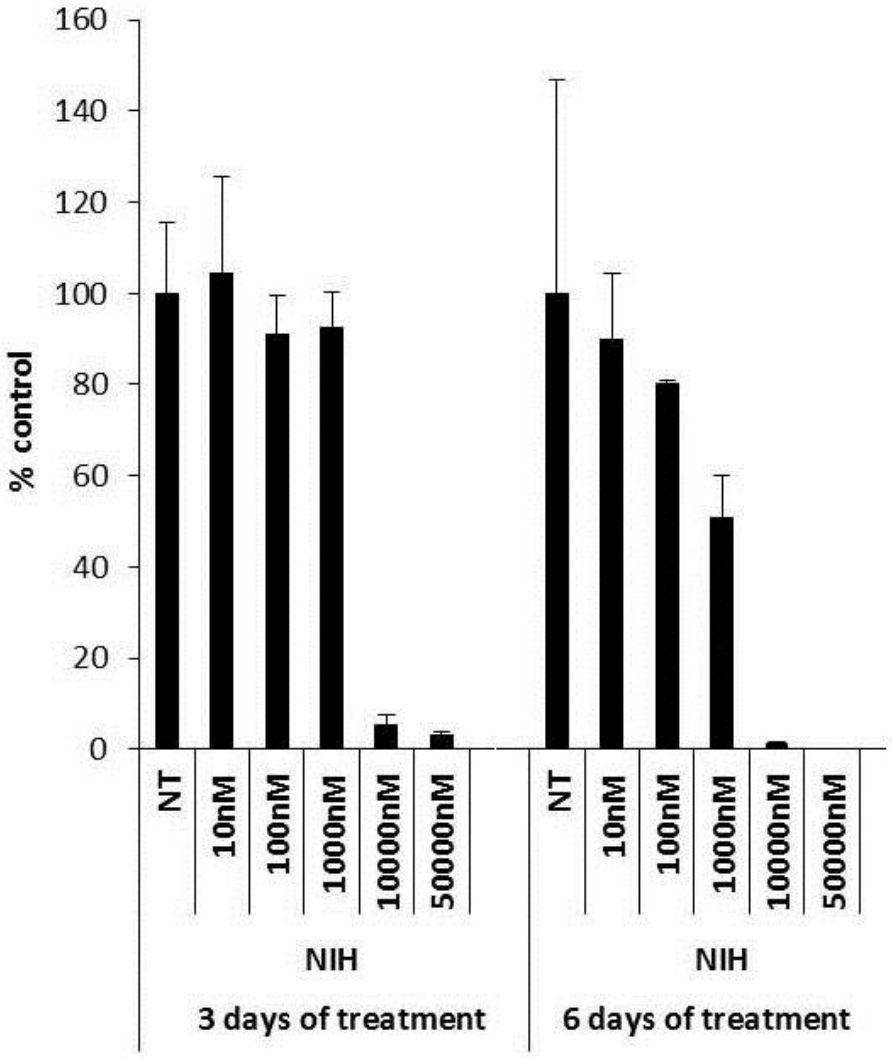

Supplemental Figure 9: Activity of Pz-1 on the proliferation of control cells.
Parental NIH3T3 fibroblasts were incubated in complete media in triplicate with vehicle (NT) or the indicated concentrations of Pz-1 and counted at the indicated time points. Cell numbers were expressed as percentage ± SD of average number of NT cells

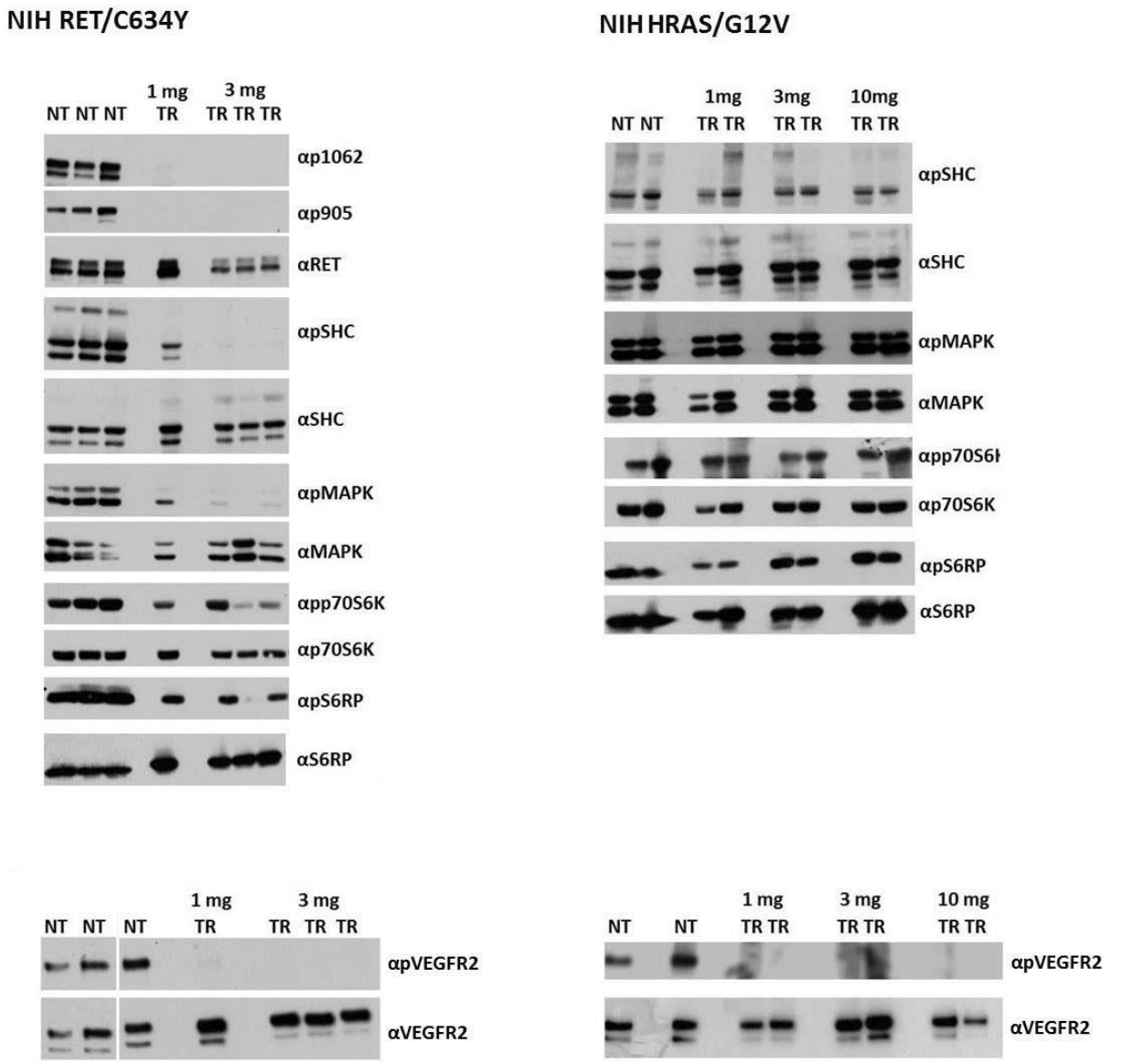

Supplemental Figure 10: Effects of Pz-1 on cellular phosphorylation events in nude mice implanted with cells transformed by RET/C634Y or HRAS/G12V.

Representative tumors from the experiment reported in Figure 4 were harvested from mice treated with indicated doses of Pz-1 (TR) or left untreated (NT), proteins were extracted and immunoblotted with the indicated antibodies.

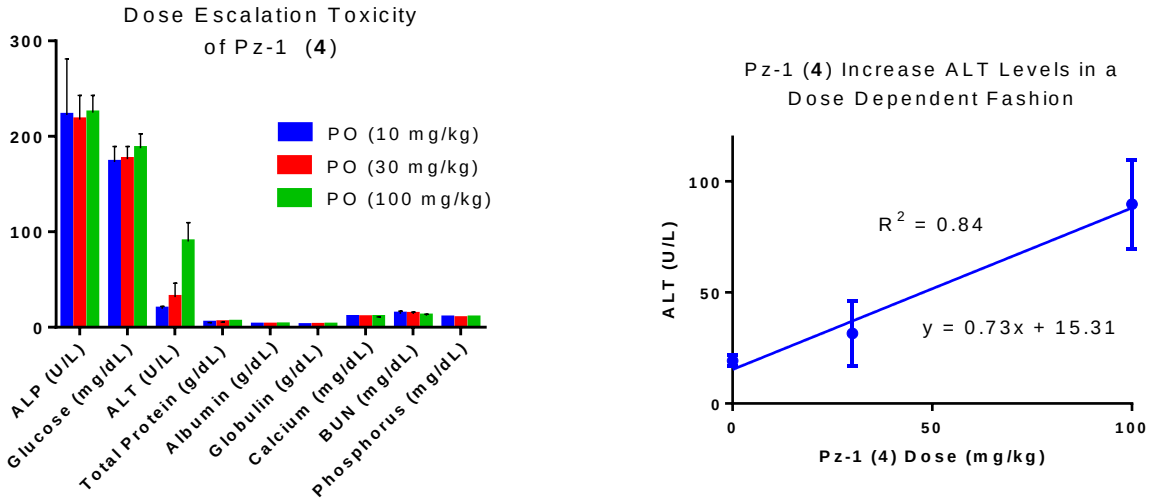

Supplemental Figure 11. Pz-1 dose escalation study in BALB/c mice.
Serum chemistry was performed for the indicated markers upon a 7 days treatment course with indicated daily PO concentrations. Alanine transaminase (ALT) fitting curve is reported in the right panel. ALT normal range for BALB/c mice is between 17-77 U/L.

Supplemental Table 1: Tumor volume formation (mm^3) with Pz-1 treatment at three weeks post tumor implantation.

Dose (mg/kg/day)	NIH3T3 RET^{C634Y}	NIH3T3 $HRAS^{G12V}$
No Treatment	974 $mm^3 \pm$ 1042 mm^3	1030 $\pm$ 1045 mm^3
1.0	0.0 mm^3 [a]	209 $\pm$ 300 mm^3 [a]
3.0	0.0 mm^3 [a]	352 $\pm$ 685 mm^3 [b]
10.0	0.0 mm^3 [a]	324 $\pm$ 346 mm^3 [a]

[a] *p*-value < 0.02, error is reported as standard deviation.
[b] *p*-value < 0.05, error is reported as standard deviation.

Supplemental Table 1. Tumor volume formation (mm^3) with Pz-1 treatment at three weeks post tumor implantation.

Pz-1 Pharmacokinetic Properties		
	IV (1.0 mg/kg)	**PO (10.0 mg/kg)**
C_0 (ng/mL)	528 ± 29.7	/
C_{max} (ng/mL)	/	2,700 ± 890
T_{max} (h)	/	2.0
$T_{1/2}$ (h)	2.86 ± 0.183	4.06 ± 0.260
$AUC_{0\text{-last}}$ (ng*h/mL)	1845 ± 505	18060 ± 3125
$AUC_{0\text{-inf}}$ (ng*h/mL)	1896 ± 453	18430 ± 3125
Bioavailability (%)	/	**97%**

Supplemental Table 2. Pz-1 pharmacokinetic properties.
Pharmacokinetic properties were determined in male Sprague-Dawley (SD) rats following a single IV bolus dose and PO administration. The entire PK study was outsourced to WuXi AppTec (Shanghai) Co., Ltd.